

**CHARACTERIZATION OF GaN NANOWIRES GROWN BY
THERMAL EVAPORATION ON DIFFERENT SUBSTRATES
AND THE STUDY OF THEIR CAPABILITY AS A SOLAR
CELL**

by

Leila Shekari

**Thesis submitted in fulfillment of the requirements
for the degree of
Doctor of Philosophy**

April 2013

ACKNOWLEDGEMENTS

Foremost, I would like to thank Allah for granting me good health and patience to complete this research. Also I would like to express sincere gratitude to my main supervisor, Prof. Dr. Haslan Abu Hassan for his intellectual guidance; devoted time and support in completing this study. I would like to send my thanks to my co-supervisor, Prof. Dr. Zainuriah Hassan for her guidance and support throughout this study. I appreciate the help of Dr. Sabah M. Thahab and Dr. Alaa Jabbar Ghazai, for their valuable suggestions, which made this work as it is.

I would also like to thank the NOR Lab staff of the School of Physics, USM for the attention and assistance they have given me since I started my PhD years.

I would like to express my gratitude to my kind husband and my dear parents, and to my dear brothers for giving me their great love, endless support, sympathy and encouragement when I needed it, during my pursuit of my doctoral study.

TABLE OF CONTENTS

LIST OF TABLES	viii
LIST OF FIGURES	ix
LIST OF ABBREVIATIONS	xiii
LIST OF SYMBOLS	xv
ABSTRAK	xviii
ABSTRACT	xx
CHAPTER 1	1
INTRODUCTION	1
1.1 Introduction to III-nitrides and Their NWs	1
1.2 Historical Development of GaN and Devices Based on GaN and Their NWs	4
1.3 Problem Statement	5
1.4 Research Objectives	6
1.4.1 Originality of the Research Works	7
1.4.2 Scope of Study	7
1.5 Outline of the Thesis	8
CHAPTER 2	9
LITERATURE REVIEW	9
2.1 Introduction	9
2.2 GaN NW Growth Techniques	9
2.2.1 GaN NWs Grown by MBE	11
2.2.2 GaN NWs Grown by HVPE	12
2.2.3 GaN NWs Grown by MOCVD	12
2.2.4 GaN NWs Grown by CVD	13
2.2.5 GaN NWs Grown by Laser-Assisted Catalytic Growth	15
2.2.6 GaN NWs Grown by Thermal Evaporation	16
2.2.6.1 Choice of Substrates	18
2.2.6.2 Type of Gases as Carriers	19
2.3 Solar Cell Based on Nitrides	21
2.3.1 Thin Film Nitrides Solar Cell	21
2.3.2 GaN NWs Solar Cell	22
2.3.3 Metal Contacts for Thin Film Nitrides Solar Cell	23

2.4 Summary	24
CHAPTER 3	25
THEORETICAL FRAMEWORK	25
3.1 Introduction	25
3.2 Energy Bands in Solids	25
3.3 Band Structure of Semiconductor	27
3.3.1 Band Structure Modification of Semiconductor Nanostructures	29
3.3.1.1 The Density of States (DOS)	32
3.3.2 Effective Mass Approximation (EMA)	34
3.4 Growth Technique	35
3.4.1 Thermal Evaporation Growth Technique	35
3.4.2 Thermal Evaporation Growth Technique for GaN NWs	36
3.4.3 GaN NWs Growth Mechanisms	36
3.5 Theory of Metal-Semiconductor Contact	39
3.5.1 Band Structures	40
3.5.2 Current Flow Mechanism	41
3.5.3 Ohmic Contact	42
3.5.4 Schottky Contact and Barrier Height	44
3.6 Principle of GaN-based Solar Cells	45
3.6.1 Solar Cells	45
3.6.1.1 Solar Cell Principle Operation	46
3.6.1.2 Solar Cell Parameters	46
3.6.1.3 Important Parameters for Efficiency	51
3.6.1.4 Solar Cell Nanostructure	52
3.6.1.4.1 Fundamentals of NW Solar Cells	52
3.7 Summary	53
CHAPTER 4	54
METHODOLOGY	54
4.1 Introduction	54
4.2 GaN NWs Syntheses	54
4.2.1 Wafer Cleaning	54
4.2.2 GaN NWs Grown by Thermal Evaporation	56
4.3 Methodology	56
4.4 Principles of the Characterization Tools	57

4.4.1 Scanning Electron Microscopy (SEM)	57
4.4.2 Energy Dispersive X-ray Spectroscopy (EDX)	58
4.4.3 High Resolution X-ray Diffraction (HR-XRD)	58
4.4.4 Photoluminescence (PL)	59
4.4.5 Transmission Electron Microscope (TEM)	60
4.5 Aluminum (Al) and Nickel (Ni) Metal Contacts	62
4.6 Fabrication and Characterization of Solar Cell	65
4.6.1 Fabrication of GaN NWs Solar Cells	65
4.6.1.1 Metallization	66
4.6.1.2 Thermal Evaporation	66
4.6.2 Solar Cell Characterization	67
4.6.2.1 Solar Simulator for Solar Cell Parameters Measurement	67
4.7 Summary	68
CHAPTER 5	69
RESULTS AND DISCUSSIONS	69
5.1 Introduction of GaN Growth on Various Substrates	69
5.1.1 GaN NWs Grown on Si (111) and Si (100)	69
5.1.1.1 Scanning Electron Microscopy (SEM)	69
5.1.1.2 Energy Dispersive X-ray Spectroscopy (EDX)	71
5.1.1.3 Transmission Electron Microscope (TEM)	72
5.1.1.4 High Resolution X-ray Diffraction (HR-XRD)	73
5.1.1.5 Photoluminescence (PL)	75
5.1.2 GaN NWs Grown on Au-Coated Silicon (111)	77
5.1.2.1 Scanning Electron Microscopy (SEM)	77
5.1.2.2 Energy Dispersive Spectroscopy (EDX)	78
5.1.2.3 Transmission Electron Microscope (TEM)	79
5.1.2.4 High Resolution X-ray Diffraction (HR-XRD)	80
5.1.2.5 Photoluminescence (PL)	81
5.1.3 GaN NWs Grown on Porous Silicon (111)	82
5.1.3.1 Scanning Electron Microscopy (SEM)	82
5.1.3.2 Energy Dispersive X-ray Spectroscopy (EDX)	83
5.1.3.3 Transmission Electron Microscope (TEM)	84

5.1.3.4 High Resolution X-Ray Diffraction (HR-XRD)	84
5.1.3.5 Photoluminescence (PL)	85
5.1.4 GaN NWs Grown on Porous GaN	86
5.1.4.1 Scanning Electron Microscopy (SEM)	87
5.1.4.2 Energy Dispersive X-ray Spectroscopy (EDX)	87
5.1.4.3 Transmission Electron Microscope (TEM)	88
5.1.4.4 High Resolution X-ray Diffraction (HR-XRD)	89
5.1.4.5 Photoluminescence (PL)	90
5.1.5 GaN NWs Grown on Porous ZnO	91
5.1.5.1 Scanning Electron Microscopy (SEM)	92
5.1.5.2 Energy Dispersive X-ray Spectroscopy (EDX)	92
5.1.5.3 Transmission Electron Microscope (TEM)	93
5.1.5.4 High Resolution X-Ray Diffraction (HR-XRD)	94
5.1.5.5 Photoluminescence (PL)	96
5.1.6 Summary of Growth on Various Substrates	97
5.2 Introduction to GaN NWs Solar Cell	98
5.2.1 Solar Cell Characterization Set-up	98
5.2.2 n-GaN NW/p-Si (111) Solar Cell	99
5.2.2.1 Scanning Electron Microscopy (SEM) of n-GaN NW/p-Si (111) Solar Cell	99
5.2.2.2 Performance of n-GaN NW/p-Si (111) Solar Cell	100
5.2.3 n-GaN NW/p-Si (100) Solar Cell	102
5.2.3.1 Scanning Electron Microscopy (SEM) of n-GaN NW/p-Si (100) Solar Cell	102
5.2.3.2 Performance of n-GaN NW/p-Si (100) Solar Cell	103
5.2.4 Summary of GaN NWs Solar Cell	106
CHAPTER 6	107
CONCLUSIONS AND FURTHER STUDIES	107
6.1 Conclusions	107
6.2 Future Studies	108
REFERENCES	110
APPENDIX A	122

APPENDIX B	124
APPENDIX C	125
PUBLICATIONS	126

LIST OF TABLES

Table 1. 1: Comparison of semiconductor material properties, at 300 K (taken from Ref [7])	3
Table 3.1: Parameters used in estimating the size of the nanocrystallites in GaN and Si (taken from Ref. [84])	35
Table 4. 1: Beaker and composition of solution	55
Table 5.1: Weight% and Atomic% of the elements detected in GaN NWs grown on Si (111)	71
Table 5.2: Weight% and Atomic% of the elements detected in GaN NWs grown on Si (100)	71
Table 5. 3: Weight% and Atomic% of the elements detected in GaN NWs grown on Au-coated Si (111)	78
Table 5. 4: Weight% and Atomic% of the elements detected in GaN NWs grown on PGaN	88
Table 5.5: Weight% and Atomic% of the elements detected in GaN NWs grown on PZnO	93
Table 5.6: Results of GaN NWs on different substrates	97
Table 5.7: AM 1.5 illuminated I-V-characteristics of n-GaN NWs solar cell on a p-Si (111) substrate	101
Table 5. 8: AM1.5 G illuminated I-V characteristics of n-GaN NWs solar cell on a p-Si (100) substrate solar cells	104

LIST OF FIGURES

Figure 1.1: Bandgap (E_g) of hexagonal AlN, GaN, and InN and their alloys; versus lattice constant a , at room temperature (taken from Ref. [2])	2
Figure 2.1: A typical MBE growth chamber (taken from Ref.[24])	11
Figure 2.2: (a) Schematic of the CVD growth tube furnace with two substrates and a gallium source in a boat within the quartz tube. During growth, the tube is closed and linked to a pump, and NH_3 enters through a mass-flow controller. (b) Schematic diagram showing the suggested VLS growth mechanism. Ga and NH_3 vapor condense in the melted Ni or Fe nanoparticles (VL process) and then crystallize at the substrate (LS condensation) [39,40]	14
Figure 2.3: Experimental setup to synthesize GaN NWs by laser ablation (taken from Ref. [24])	16
Figure 2.4: The overall evolution of NW growth following the production of the catalytic nanocluster using laser ablation (taken from Ref. [42])	16
Figure 2.5: Scheme of the experimental-growth setup (taken from Ref. [46])	17
Figure 2.6: Schematic of the Ag/n- $Al_xIn_yGa_{1-(x+y)}N$ /AlN(buffer)/p-Si/Au solar cell. (taken from Ref.[70])	24
Figure 3.1: Electron band (a) in single atom, (b) in five closed atoms, (c) overlap in metals, (d) separation in semiconductors, and (e) separation in insulators (taken from Ref. [76])	26
Figure 3.2: The first Brillouin zone of the FCC	27
Figure 3.3: Schematic diagram of the valence band and direct/indirect bandgap conduction bands. The solid line indicates the conduction band of the direct bandgap semiconductor, whereas the dashed line represents the conduction band of the indirect bandgap semiconductor (taken from Ref. [80])	28
Figure 3.4: A NW with rectangular cross section with the potentials in y- and z- directions	29
Figure 3.5: 1D system, Z is the growth direction (taken from Ref. [78])	33
Figure 3.6: Schematic diagram illustrating the electronic DOS of a 3-, 2-, 1-D system, (taken from Ref. [85])	34
Figure 3.7: Schematic illustration for the growth mechanism of GaN NWs [94].	37
Figure 3.8: Schematic illustration of the growth mechanism: (a) Au-coated Si wafer before growth; (b) wafer during heating of the sample, creation of Au droplets; (c) formation of GaN droplets directly after putting the source	

material; (d) growth and solidification of the NWs under the GaN droplets	39
Figure 3.9: (a) Metal and p-type semiconductor (b) Metal and n-type semiconductor, before and after linking together, without any surface/interface states (taken from Ref [102])	40
Figure 3.10: Schematic representation of a p-n junction under illumination (taken from Ref. [106])	42
Figure 3.11: Conduction mechanisms for metal/n-semiconductor ohmic contacts (taken from Ref. [107])	43
Figure 3.12: Conduction mechanisms for metal/n-semiconductor Schottky contacts (taken from Ref. [107])	44
Figure 3.13: Schematic diagram of a solar cell (taken from Ref.[114])	45
Figure 3.14: J-V characteristic of an ideal diode in the dark and in the light. The net current is achieved by adjusting the bias voltage-dependent dark current up to a constant amount similar to that of the short-circuit photocurrent (taken from Ref.[109])	47
Figure 3.15: Equivalent circuit of an ideal solar cell. (taken from Ref.[109])	48
Figure 3.16: Current-voltage (black) and power-voltage (grey) diagrams of an ideal cell. The density of the power reaches a maximum at V_m , which is close to V_{oc} . The maximum power density $J_m \times V_m$ is also given by the surface area of the inner rectangle. The outer rectangle has an area of $J_{sc} \times V_{oc}$. If FF is equal to 1, the current-voltage curve follows the outer area of the rectangle (taken from Ref. [109])	49
Figure 3.17: Equivalent circuit, for a real solar cell, including series and shunt resistances (taken from Ref. [109])	50
Figure 3.18: Effect of (a) increasing series, and (b) reducing parallel resistances. The outer curve has $R_s = 0$ and $R_{sh} = \infty$, in each cases.(taken from Ref.[109])	50
Figure 4.1: Flow of RCA cleaning process (taken from Ref.[33])	56
Figure 4.2: A schematic figure of the furnace and its components	57
Figure 4.3: X-ray beam projected onto the sample at an angle θ	59
Figure 4.4: Schematic of ray diagram for a TEM (taken from Ref. [121])	61
Figure 4.5: Schematic diagrams which show the formation mechanism of Al/Ni droplets on GaN NWs by furnace annealing: (a) Al/Ni nanoparticles deposited by thermal evaporation technique are attached on the surface of a GaN NWs, (b) diffusion of Al/Ni nanoparticles into GaN NWs under	

heating, (c) combination of Al/Ni molecules and diffuse into GaN NW at elevated temperature (e.g. 800 °C)	63
Figure 4.6: Image of Si substrate containing GaN NWs with the metal contacts Arrows indicate the size of metal contact on the GaN NWs	64
Figure 4.7: The schematic diagram of GaN NWs with Al/Ni metal contacts	65
Figure 4.8: A schematic diagram of n-GaN NWs on p-Si solar cell	66
Figure 4.9: Schematic diagram of a power measurement by a Solar Simulator	68
Figure 5.1: SEM image of GaN NWs deposited on the Si (111) substrate	70
Figure 5.2: SEM image of GaN NWs deposited on the Si (100) substrate	70
Figure 5.3: EDX spectra of GaN NWs on Si (111)	71
Figure 5.4: EDX spectra of GaN NWs on Si (100)	71
Figure 5.5: TEM image of GaN NWs grown on Si (111) substrate	73
Figure 5.6: TEM image of GaN NWs grown on Si (100) substrate	73
Figure 5.7: HR-XRD spectrum of the synthesized GaN NWs on the Si (111) substrate	74
Figure 5.8: HR-XRD spectrum of the synthesized GaN NWs on the Si (100) substrate	75
Figure 5.9: PL spectrum of the GaN NWs on the Si (111) substrate at room temperature (300K)	76
Figure 5.10: PL spectrum of the GaN NWs on the Si (100) substrate at room temperature (300K)	76
Figure 5.11: SEM images of GaN NWs deposited on Au-coated Si (111) substrate from top view at (a) 10K and (b) 50K magnifications	77
Figure 5.12: EDX image of GaN NWs on Au-coated Si (111) substrate	78
Figure 5.13: TEM image of GaN NWs	79
Figure 5.14: HR-XRD spectrum of synthesized GaN NWs on Au-coated Si (111) substrate Note: Unknown peaks are indicated in *	80
Figure 5.15: PL spectrum of GaN NWs on Au-coated Si substrate at room temperature (300K)	81
Figure 5.16: SEM image of GaN NWs grown on PS substrate from top view at (a) 2K and (b) 10K magnifications	82
Figure 5.17: EDX spectra of GaN NWs grown on PS substrate	83
Figure 5.18: TEM image of a GaN NW	84

Figure 5.19: HR-XRD spectrum of GaN NWs on PS substrate	85
Figure 5.20: PL spectrum of GaN NWs on PS	86
Figure 5.21: SEM image of GaN NWs on PGaN substrate	87
Figure 5.22: EDX spectra of (a) PGaN and (b) GaN NWs	88
Figure 5.23: TEM image of GaN NW	89
Figure 5.24: X-ray diffraction of the (a) as-grown PGaN and (b) GaN NWs on PGaN substrate	90
Figure 5.25: PL spectrum of the (a) as-grown PGaN and (b) GaN NWs on the PGaN substrate, at room temperature (300K)	91
Figure 5.26: SEM image of GaN NWs	92
Figure 5.27: EDX spectrum of GaN NWs on PZnO	93
Figure 5.28: TEM image of a GaN NW	94
Figure 5.29: HR-XRD of the (a) as-grown PZnO wafer, and (b) GaN NWs	95
Figure 5.30: PL spectrum of the (a) as-grown PZnO wafer, and (b) GaN NWs, at room temperature (300K)	96
Figure 5.31: Schematic representation of the NWs of n-GaN/p-Si heterojunction solar cell	98
Figure 5.32: SEM image of n-GaN NWs on p-Si (111) substrate (a) top view at 4K magnification, (b) top view at 10K magnification and (c) cross sectional view	100
Figure 5.33: Current-voltage characteristics of n-GaN NWs/p-Si (111) solar cell; (a) a-electrode is Ni and b-electrode is Al, (b) both electrodes are Ni, (c) a-electrode is Al and b-electrode is Ni, (d) both electrodes are Al	102
Figure 5.34: SEM image of n-GaN NWs on p-Si (100) substrate (a) top view at 4K magnification, (b) top view at 10K magnification and (c) cross sectional view	103
Figure 5.35: Current-voltage characteristics of NWs of n-GaN/p-Si (100) solar cells; (a) a-electrode is Ni and b-electrode is Al, (b) both electrodes are Ni, (c) a-electrode is Al and b-electrode is Ni, (d) both electrodes are Al	105

LIST OF ABBREVIATIONS

AM	Air mass
ARC	Antireflection coating
CVD	Chemical vapor deposition
CBE	Chemical beam epitaxy
DOS	Density of states
EDX	Energy dispersion X-ray
EMA	Effective Mass Approximation
EQE	External quantum efficiency
FCC	Face-centered cubic
FF	Fill factor
FWHM	Full width at half maximum
HPT	Hot probe technique
HR-XRD	High resolution X-ray diffraction
HVPE	Hydride vapor phase epitaxy
IQE	Internal quantum efficiency
I-V	Current-voltage
LD	Laser diode
LDOS	Local density of states
LED	Light emitting diode
LS	Liquid solid

MBE	Molecular beam epitaxy
MOCVD	Metal organic chemical vapor deposition
MOVPE	Metal-organic vapor phase epitaxy
MQW	Multi-quantum well
MS	Metal-semiconductor
PD	Photodetector
PL	Photoluminescence
PV	Photovoltaic
QE	Quantum efficiency
RCA	Radio Corporation of America
RF-PAMBE	Radio-frequency plasma- assisted molecular beam epitaxy
SEM	Scanning electron microscopy
STC	Standard test condition
TEM	Transmission electron microscope
UV	Ultraviolet
VLS	Vapor–liquid–solid
VPE	Vapor phase epitaxy
VS	Vapor solid

LIST OF SYMBOLS

a	Lattice constant
A^*	Effective Richardson constant
a_o, c_o	Unstrained lattice constant
d	Interplaner space of the diffraction planes
D	Dimension
E	Electric field
E_0	Ground state of quantum well system
E_{BR}	Breakdown Field
E_c	Conduction band edge
E_F	Fermi level of semiconductor
E_{FM}	Fermi energy in the metal
E_{FS}	Fermi energy in the semiconductor
E_v	Valence band edge
E_g	Bandgap energy
$E_g^{nano}(R)$	Effective bandgap of a particle with radius R
E_n	Quantized-states energies
eV	Electron volt
F_m	Fermi-Dirac distribution function for metal
F_s	Fermi-Dirac distribution occupational probability for semiconductor
$g(k)$	Density of states of electrons per unit k point
I	Current

I_{dark}	Dark current
I_m	Maximum current
I_{sc}	Short-circuit current
j	Current density
J_{dark}	Dark current density
J_{ms}	Current traversing from metal to semiconductor
k	Space wave vector
k_B	Boltzmann's constant
m^*	Effective mass of the tunneling carriers
m_e^*	Effective mass of the electron in the conduction band
m_h^*	Effective mass of the hole in the valence
N_d	Doping concentration
$P(E)$	Probability of the tunneling
P_m	Maximum power output
P_s	Power density of the incident light
q	Electron charge
R	Radius of particle
R	Resistance
R_c	Contact resistance
$sccm$	Standard cubic centimeters per minute
t	Time
T	Absolute temperature
$T(\xi)$	Quantum transmission coefficient above the potential maximum

$T(\eta)$	Quantum transmission coefficient below the potential maximum
V	Voltage
V_m	Maximum voltage
V_{oc}	Open-circuit voltage
x_d	Barrier width
v_s	Velocity
ϵ	Dielectric constant
δ	Dislocation density
θ	Diffraction angle
χ_s	Electron affinity
η	Efficiency
\hbar	Plank's constant
λ	Wavelength
μ	Carrier mobility
ρ_c	Specific contact resistivity
ϕ	Work function
Φ_B	Energy needed by an electron at the Fermi level in the metal to enter the conduction band of the semiconductor
Φ_{Bn}	Metal-semiconductor barrier height
ϕ_m	Work function of metal
ϕ_s	Work function of semiconductor
$\Omega.cm$	Ohm centimeter

**PENCIRIAN NANODAWAI GaN YANG DIHASIL
MENGUNAKAN PENYEJATAN TERMA DI ATAS SUBSTRAT
BERBEZA DAN KAJIAN KEUPAYAAN MEREKA SEBAGAI
SEL SURIA**

ABSTRAK

Dalam kajian ini, nanodawai (NWs) galium nitrida (GaN) dihasilkan di atas substrat berbeza, seperti Silikon (Si) (111) dan (100) sama ada dengan atau tanpa lapisan Emas (Au), Si Berliang (PS), GaN Berliang (PGaN) dan ZnO Berliang (PZnO), menggunakan kaedah Penyejatan Terma.

Imej SEM bagi NWs GaN yang telah disintesis mempamerkan pandangan atas NWs GaN yang kelihatan mempunyai ketumpatan tinggi dan bertertib lurus bagi substrat Si (111) dibandingkan dengan NWs GaN di atas substrat Si (100). Imej SEM bagi NWs GaN di atas Si (100), Si (111) dilapisi Au dan PZnO menunjukkan ketumpatan NWs kelihatan kurang daripada ketumpatan NWs di atas substrat yang lain.

Tiada bendasing dikesan dalam spektra EDX bagi NWs GaN yang dihasilkan di atas substrat Si (111), Si (100), PS dan PGaN, kecuali bagi Oksigen (O). Sementara analisa EDX bagi NWs GaN di atas Si (111) dilapisi Au menunjukkan kehadiran bendasing Oksigen (O) dan Karbon (C), yang menandakan bahawa penggunaan mungkin menghasilkan kontaminasi menerusi kaedah ini.

Corak HR-XRD bagi endapan NWs GaN di atas Si (111), Si (100), PGaN, PS dan PZnO mengesahkan pembentukan habluran NWs GaN. Ini menandakan bahawa sampel mempunyai ketulenan yang tinggi. Puncak HR-XRD mendedahkan bahawa

NWs GaN di atas substrat Si (111) dilapisi Au tidak mempunyai kualiti habluran tinggi jika dibandingkan dengan NWs GaN yang dihasilkan di atas substrat yang lain, kerana mempunyai bendasing Ga_2Au dan Ga_2O_3 .

Rajah TEM menunjukkan bahawa nanostruktur GaN di atas semua substrat berbentuk NWs. NWs ini terdiri daripada sel swahimpunan dengan diameter yang agak seragam dihasilkan di sepanjang paksi dawai.

Puncak PL mewakili gabungan semula jalur ke jalur di dalam NWs GaN yang ditumbuhkan di atas Si (111) dan Si (100). Puncak PL bagi NWs GaN di atas substrat Si (111) dilapisi Au menunjukkan satu penambahan bilangan pusat luminesens, yang mungkin disebabkan oleh bendasing di dalam NWs bagi sampel ini.

Akhirnya lapan sel suria simpang-tunggal disediakan menggunakan sampel dengan kombinasi sentuhan logam tersepuh lindap ($800\text{ }^\circ\text{C}$), yang terdiri daripada Al/n-GaN/p-Si/Al, Al/n-GaN/p-Si/Ni, Ni/n-GaN/p-Si/Al and Ni/n-GaN/p-Si/Ni, menggunakan kedua-dua substrat p-Si (111) dan p-Si (100). Sel suria Ni/n-GaN/p-Si(100)/Al mempunyai kecekapan penukaran suria tertinggi 10.7%, bagi sel $0.3 \times 0.3\text{ cm}^2$ dibawah simulasi pencahayaan AM1.5.

CHARACTERIZATION OF GaN NANOWIRES GROWN BY THERMAL EVAPORATION ON DIFFERENT SUBSTRATES AND THE STUDY OF THEIR CAPABILITY AS A SOLAR CELL

ABSTRACT

In this study, Gallium Nitride (GaN) nanowires (NWs) were grown on different substrates, such as Silicon (Si) (111) and (100) either with or without Gold (Au) coating, Porous Si (PS), Porous GaN (PGaN) and Porous ZnO (PZnO), using the Thermal Evaporation method.

SEM images of the synthesized GaN NWs displayed an overview of apparently high density and straight well-ordered GaN NWs on the Si (111) substrate compare to GaN NWs on Si (100) substrate. The SEM images of GaN NWs on Si (100), Au-coated Si (111) and PZnO indicated that the density of NWs was apparently less than that in samples of other substrates.

No impurities were detected in the EDX spectra of the GaN NWs grown on Si (111), Si (100), PS and PGaN substrates, except for Oxygen (O). While the EDX analysis of the GaN NWs on Au-coated Si (111) indicates the presence of O and Carbon (C) impurities, suggesting that the usage of catalyst causes contamination by this method.

The HR-XRD patterns of the deposited GaN NWs on Si (111), Si (100), PGaN, PS and PZnO confirmed the formation of crystalline GaN NWs. This indicated that the samples were of high quality. The HR-XRD peaks revealed that GaN NWs on Au-coated Si (111) substrate were not of high crystalline quality compare to those grown on other substrates, with Ga_2Au and Ga_2O_3 impurities.

The TEM figures showed that the GaN nanostructures on all substrates were in the shape of NWs. These NWs were composed of self assembly cells with rather uniform diameter growing along the wire axis.

The PL peaks represented band to band recombination in GaN NWs grown on Si (111) and Si (100). The PL peak of GaN NWs on Au-coated Si (111) substrate showed an increase of the number of luminescent centers, which could be due to the contaminations inside the NWs for this sample.

Finally eight single-junction solar cells were prepared using samples with annealed (800 °C) metal contacts combinations, consisting of Al/n-GaN/p-Si/Al, Al/n-GaN/p-Si/Ni, Ni/n-GaN/p-Si/Al and Ni/n-GaN/p-Si/Ni, using both p-Si (111) and p-Si (100) substrates, respectively. The Ni/n-GaN/p-Si(100)/Al solar cell had the highest solar conversion efficiency of 10.7%, for a $0.3 \times 0.3 \text{ cm}^2$ cell under simulated AM1.5 illumination.

CHAPTER 1

INTRODUCTION

1.1 Introduction to III-nitrides and Their NWs

For the last three decades, the III–V semiconductor materials have been viewed significantly promising for semiconductor applications from blue to UV wavelengths in the same manner that the highly successful P-based and As-based counterparts have been used for infrared from red to yellow wavelengths. The III–V nitride family members, namely, InN, GaN, AlN, and their alloys, are wide bandgap materials; they can crystallize in either wurtzite or zincblende polytypes. Figure 1.1 shows that wurtzite InN, GaN, and AlN with direct bandgaps, from ~ 0.7 eV to 6.2 eV at room temperature. In addition, InN, and GaN in cubic form have direct bandgaps, whereas AlN is indirect. Among these wide and direct bandgap materials, GaN alloyed with InN and AlN may span an allied range of direct band gaps throughout much more of the visible spectrum into the UV wavelengths. This makes the III-nitride system more interesting for optoelectronic device applications, such as detectors, LDs, and LEDs, which are active in UV, blue, or green wavelengths [1].

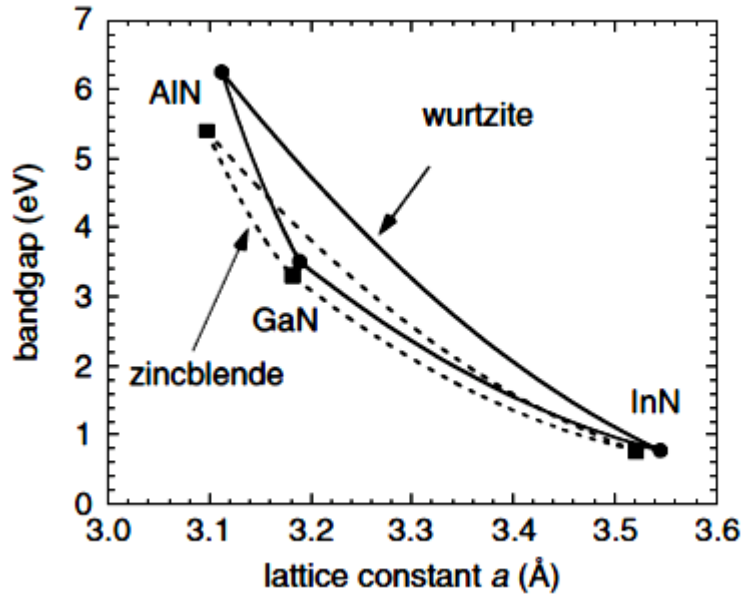


Figure 1.1: Bandgap (E_g) of hexagonal AlN, GaN, and InN and their alloys; versus lattice constant a , at room temperature (taken from Ref. [2])

The addition of III–V nitrides to the family of device-quality semiconductors is essential in developing color displays and coherent sources for dense optical storage technologies, and similar devices for illumination application. Another area in which III–V nitrides have gained much attention is high power/high temperature electronics [3]. The first one is their natural wide bandgap. The III–V nitrides, such as GaN, can be used for high temperature applications because they can be intrinsic at much higher temperatures than other semiconductors, such as GaAs, Si, and Ge. The second fascinating property of III–V nitrides is their high breakdown fields. This critical electric field scales with the square of the energy bandgap (E_g^2) and is estimated to have a volume for more than 4 MV/cm for GaN compared to 0.2 MV/cm and 0.4 MV/cm for Si and GaAs, respectively [4, 5].

Table 1.1 shows that GaN also has extraordinary electron transport properties, including high saturated drift velocity and good mobility [6]. These characteristics make GaN suitable for general electronics, especially microwave rectifiers. The material

properties of GaN and some conventional semiconductors are listed in Table 1.1. GaN can be expected to demonstrate eventually its superiority over other semiconductors in this area. The strongest emphasis of III–V nitrides, compared with SiC, is the heterostructure technology it can support. Heterojunction structures, modulation doped hetero-interface, and quantum well can be made in this system; which gives access to new operation procedures for electronic devices and new spectral areas for optical devices. This feature can make III–V nitrides applicable as wide band-gap systems, which have set the modern criterion for microwave devices.

Thermal stability and high mechanical properties, the possibility of passivation, and large piezoelectric constants are other advantages of III–V nitrides [5].

Table 1. 1: Comparison of semiconductor material properties, at 300 K (taken from Ref [7])

Properties	GaN	Si	SiC
E_g (eV)	3.4	1.12	3.2
E_{BR} (MV/cm)	3.3	0.3	3.5
v_s ($\times 10^7$ cm/s)	2.5	1.0	2.0
μ (cm^2/v_s)	990-2000	1500	650

The use of Si and GaAs has been restricted, due to their theoretical limits, whereas nitrides have begun to show their promise in the past 30 years [5]. III-nitrides, such as InN, GaN, and AlN semiconductors, formed via a continuous alloy system, have been intensely studied in recent years for their potential applications.

Currently, nanostructures, such as nanowires (NWs), nanorods, and nanoparticles, are under active examination as components for PV devices. Nanostructures can potentially explore new device concepts and increase the efficiency of low-cost processed solar cells [8].

Most of the literature is focused on the development of III-nitride thin-films. Recently, considerable interest in NWs has emerged [2,7].

NWs are wire-like structures with diameters usually ranging from one nanometer to a few hundred nanometers. NWs include virtually every semiconductor system, such as III-Vs, have been synthesized in recent years and have been found to exhibit a variety of morphologies, including cylindrical, triangular, rectangular, and hexagonal [10].

1.2 Historical Development of GaN and Devices Based on GaN and Their NWs

Wurtzite GaN is a technologically important III-V semiconductor due to its excellent optoelectronic properties. It is potentially useful in blue and UV light emission, with excellent thermal stability and high mobility. It has great potential in broad commercial applications, such as UV or blue emitters, detectors, high-temperature/high-power electronic devices, and high-speed field-effect transistors. GaN NWs are promising building blocks with potential applications in nanodevices with excellent performance, such as lasers, LEDs, solar cells, and piezoelectric nanogenerator [9,10].

In the last decade, GaN-based materials have been very surprising, from their initial progress in LEDs to LDs, solar-blind UV detectors to microwave power electronics, and to solid-state UV light sources and white lighting [5]. Nowadays, there are newer areas for GaN research and development, such as megawatt electronics, sensors, spin-transport electronics (or spintronics), and gate dielectrics for transistors [1].

GaN and its alloys are technologically important direct bandgap semiconductors, which absorb and emit a broad energy from UV-visible wavelengths. Moreover, they are the basis for several commercial products. As such, NWs based on GaN are being

studied for potential use in lasers, LEDs, water splitting, high speed/power electronics, and photovoltaics [13- 16].

Great efforts have been made to fabricate well aligned 1-D NWs and NW arrays for PV device applications based on top-down or bottom-up techniques [15]. NW solar cells based on a single NW or NW arrays have been theoretically and empirically demonstrated using groups IV, III–V, or II–VI compound semiconductors, allowing the emergence of semiconductor NWs as building blocks for PV devices [16].

1.3 Problem Statement

Energy production is one of the most important problems that mankind will face in the next century. Therefore, many organizations all over the world are searching for fuels that are clean, sustainable, and low cost. For example, the US has spent more than USD 5 billion on research related to cleaner and alternative energy. One of the fastest growing renewable energy sources is solar energy. Solar energy is produced with almost zero carbon-emission and is, therefore, one of the best solutions to modern energy issues [17]. However, solar power still shares less than 0.1% of worldwide energy generation due to its high production cost [18].

On the other hand, a large variety of nanomaterial and thin film technologies have been studied for their potentially low-cost production because they use up less materials, and their higher performance than the current Si technology. In particular, semiconductor NWs offer the advantages of higher light absorption, efficient carrier segregation and collection at electrodes, and low-cost processing using fewer materials, compared with conventional PV devices [16].

Meanwhile, the requirement for global energy is increasing due to the growth of both the emerging economies of the Earth and the existing one; there is a new demand for new solar cells that could provide clean and renewable energy.

Nowadays, the primary focus of photovoltaic cell research is finding new materials and methods to reduce the cost and improve efficiency of the device [19].

Photons with an energy lower than the bandgap escape unabsorbed; photons with higher energy are absorbed, but most of their energy is wasted as heat. Crystalline silicon, the leading solar cell material, has a bandgap of only about 1.1 eV; most solar photons are much more energetic. Crystalline-silicon solar cells are approximately 25% efficient, at best.

Different materials with different bandgaps can be stacked to capture photons with a wider range of energies. In a multijunction solar cell, the top junction captures high-energy photons, whereas others pass through to the lower-bandgap junctions below [20].

As a result, the primary focus of current photovoltaic cell research is to find new methods and materials to improve device efficiency, cost, and safety.

1.4 Research Objectives

This work focuses on solving three main problems which are:

- To search for an inexpensive, but controllable method to grow high quality GaN NWs on six different substrates, such as Si (111), Si (100), Au-coated Si, PSi, PGaN and PZnO.
- To conduct structural, morphological and optical characterizations of the grown GaN NWs.

- To fabricate GaN NWs photovoltaic materials on Si (111) and Si (100) substrates. This approach may lead to solar cells that are cheaper than the photovoltaic cells to date. These NWs can create a surface that is able to absorb more sunlight than a flat surface, thus improving cell efficiency [21]. Therefore, using GaN NWs, instead of GaN thin film, can improve the efficiency of cells.

1.4.1 Originality of the Research Works

1. The GaN NWs are prepared by Thermal Evaporation method, which is believed to have never been done before using just Ar gas as the carrier.
2. Using different substrates to produce GaN NWs of different diameter sizes and orientations by thermal evaporation. Different porous substrates, i.e. PSi, PGaN, PZnO, used in this project has never been reported before.
3. Fabrication of n-GaN NWs on p-Si as solar cells, to the best of our knowledge has never been performed. The thermal evaporation process is promising for solar cell manufacturing due to its simplicity, lower cost and suitability for mass production.

1.4.2 Scope of Study

The scope of this thesis is to grow GaN NWs by a simple thermal evaporation method. This research is trying to decrease the cost and the complexity of GaN NWs growth on various substrates.

This work starts with the deposition of GaN NWs on six different substrates (Si (111), Si (100), Au-coated Si, Porous Si (PSi), Porous GaN (PGaN) and Porous ZnO (PZnO). Then the morphology of each sample will be characterized using SEM and TEM. Optical, elemental and structural characterizations will also be carried out, using PL, EDX and HR-XRD, respectively.

In the next part of this work eight different single-junction solar cells will be prepared using the thin films of GaN NWs with metal contacts combinations of Al/n-GaN/p-Si/Al, Al/n-GaN/p-Si/Ni, Ni/n-GaN/p-Si/Al and Ni/n-GaN/p-Si/Ni, either using Si (111) or Si (100) substrates. Finally these solar cells will be characterized by a solar simulator under simulated AM1.5 illumination.

1.5 Outline of the Thesis

The content of this thesis is organized as follows:

In **Chapter 1** a brief introduction and development of NWs and GaN NWs and also some applications of NWs semiconductor materials are introduced.

Chapter 2 includes a literature review of the GaN NWs synthesis, as well as the general properties of III-V semiconductors groups are presented. Synthesis (preparation) of NWs materials by Thermal Evaporation technique and solar cell based on GaN is discussed.

In **Chapter 3** NWs semiconductors formation mechanisms, theory of band structure of semiconductor and principle of GaN-based devices are covered in this chapter.

Details on the methodology of the growth and general principles of operation of the instruments are discussed in **Chapter 4**.

The GaN NWs results obtained with Thermal Evaporation method on Si (111), Si (100), Porous Silicon, Au-Coated Silicon, Porous GaN and Porous ZnO and the performance of the solar cell fabricated based on GaN NWs are analyzed and discussed in **Chapters 5**.

In **Chapter 6** the conclusion and future works are discussed.

CHAPTER 2

LITERATURE REVIEW

2.1 Introduction

This chapter includes a review of GaN NW growth using different techniques, such as MBE, HVPE, MOCVD, CVD, Laser-Assisted catalytic growth and thermal evaporation. It also contains a review on different substrates and carrier gases which are usually used to grow GaN NWs.

The following sections consist of thin film nitrides solar cells, GaN NWs solar cells, and metal contacts for thin film nitride solar cells that can optimize the external quantum efficiency of the cells.

2.2 GaN NW Growth Techniques

Techniques to produce NWs are normally divided into top-down and bottom-up methods. NWs that can be produced by lithographically carving out the structures from the desired bulk material are referred to as top-down production. The major disadvantage of this method is that the surfaces of the structures are spoiled during the process, resulting in NWs with poor crystal quality [22]. Furthermore, the technique may not be able to produce sufficiently small structures.

The bottom-up methods used to produce NWs are usually grouped into solution methods and vapor phase methods. Solution methods offer poor control over NW positioning and dimensions, the properties that are very important for device applications. Electrochemical deposition also has the disadvantage of producing generally poor NW crystal quality with many defects [23]. This is a major limitation in device applications, especially in the field of optics.

Vapor phase methods are extensively used for NW production. They include physical methods, such as catalytic reaction based on a vapor–liquid–solid mechanism, direct reaction of metal gallium with ammonia, and thermal chemical vapor deposition (CVD), and epitaxial methods such as molecular beam epitaxy (MBE) [23-28]. Vapor phase methods have very important advantages. Firstly, a huge amount of vapor phase precursors exist, making it possible to grow NWs using many different types of materials. Secondly, a better control of the growth process is possible, enabling the growth of complex NW structures.

Epitaxial NW growth means that a substrate with a specific crystal structure is used to orient the growth of the NW crystal in an ordered manner and that the diameter of the seed particle (gold particle) typically determines the diameter of the NW. In most cases, the seed particle consists of gold.

However, several growth models have been developed to account for the catalyst-induced approach. Nevertheless, recent papers have pointed out that the NW contamination by the catalyst considerably limits their structural and optical quality [25].

However, vast majority of NWs are grown by the CVD, MBE, metal-organic chemical vapor deposition (MOCVD), and the laser ablation method through the conventional VLS synthesis route consumption. The key component of NWs growth is the seed, which assists the nucleation and designs the generation of NWs [26].

2.2.1 GaN NWs Grown by MBE

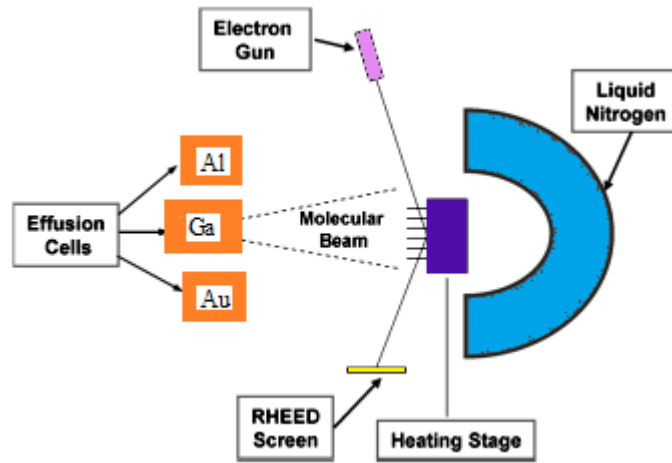


Figure 2.1: A typical MBE growth chamber (taken from Ref.[27])

Figure 2.1 shows a simplified schematic diagram of the growth chamber of an MBE system. Since the year 2000, MBE technique with ultra-high vacuum conditions has been employed to synthesize III–V [28] compound semiconductor NWs based on the VLS mechanism. This technique provides an ideal clean growth environment, and the junctions (or heterostructures), doping states, and atomic structures can be well controlled, producing high-quality semiconductor NWs.

Very recently, an extensive generalized dynamic model has been suggested by Dubrovskii et al. [28] for Au particle-assisted MBE growth of III–V NWs. GaN NWs have been grown using RF-PAMBE on Si (111), [12,31]. GaN NWs with good crystal quality [30] have been grown by MBE on various substrates. While the NWs growth by MBE has been established, a number of ambiguities remain on the mechanisms directing the growth of NWs [31,33]. Defect density and growth direction in the NWs grown by MBE are influenced by different factors. Twinning or stacking faults are the commonly observed defects that often occur in thicker NWs and can change the NW

growth direction. In addition, MBE is a very expensive growth method, which makes scientists search for other growth techniques to produce III-nitride NWs [31,34].

2.2.2 GaN NWs Grown by HVPE

In 1969, Maruska et al. reported the first Hydride vapor phase epitaxy (HVPE) of GaN using sapphire as substrate. In the 1990s, the growth of a smooth surface GaN using the HVPE method attracted the attention to produce freestanding GaN wafers [33].

HVPE is a growth technique known for a long time, where a halide vapor precursor, for example GaCl, and a hydride, like NH₃, are utilized as the precursors for groups III and V, respectively. The HVPE method can achieve a high crystal quality caused by thermal stability of the halide source, a high migration of halide molecules, and the use of high purity precursors without containing carbon. Therefore, the HVPE growth method attracts the attention employed for thick film growth method.

Recently, the growth of GaN NWs on Au/Si using HVPE has been reported with poor quality GaN nanostructures. The growth is dependent on the Ga vapor pressure and the amount of Au on the substrate. The report also mentioned that, there is no chance of depositing GaN NWs on plain Si wafer [33,36,37]. Furthermore, GaN NW growth without using catalyst has not been reported in this method.

2.2.3 GaN NWs Grown by MOCVD

The MOCVD method was used by Nichia Inc. to fabricate III–V nitride LEDs and lasers [36]. MOCVD method forms thick and thin GaN NWs through a VLS growth mechanism. The total time of NW growth takes place within a few minutes. The samples include nonuniform distributions of NWs containing areas with clean GaN

surface [37]. MOCVD templates on foreign substrates can be used widely as seeds to develop the crystal growth.

More research yielded nonpolar films with too rough and/or faceted layers for device growth. This explanation was used by Craven et al.'s MOCVD growth of smooth a-plane GaN films [29,34]. The growth is based on a VLS process and a catalyst and ammonia carrier gas are needed. Mostly, Ni thin films are utilized as catalyst for the growth of GaN NWs. Gallium metal and GaN powder has been used as Ga source. The temperature of the growth is 1150 °C, [29,35]. To avoid a catalyst-induced infection that may affect the electronic properties of the products, catalyst-free growth is preferable [40].

2.2.4 GaN NWs Grown by CVD

The VLS process in CVD growth method was developed by Wagner [41] and has been a widely used method for producing 1-D nanostructures from various inorganic materials. Han et al. [42] reported the first GaN nanorods using CVD prepared in a carbon nanotube-confined reaction. The gold catalyst for GaN NWs grown with this method needs only to be of small amount. GaN NWs, grown by CVD using Ga as a precursor, can be achieved at temperatures higher than 950 °C [42]. The schematic diagram of Figure 2.2(a) shows the furnace (3-zone 1200 °C furnace) for the CVD growth process.

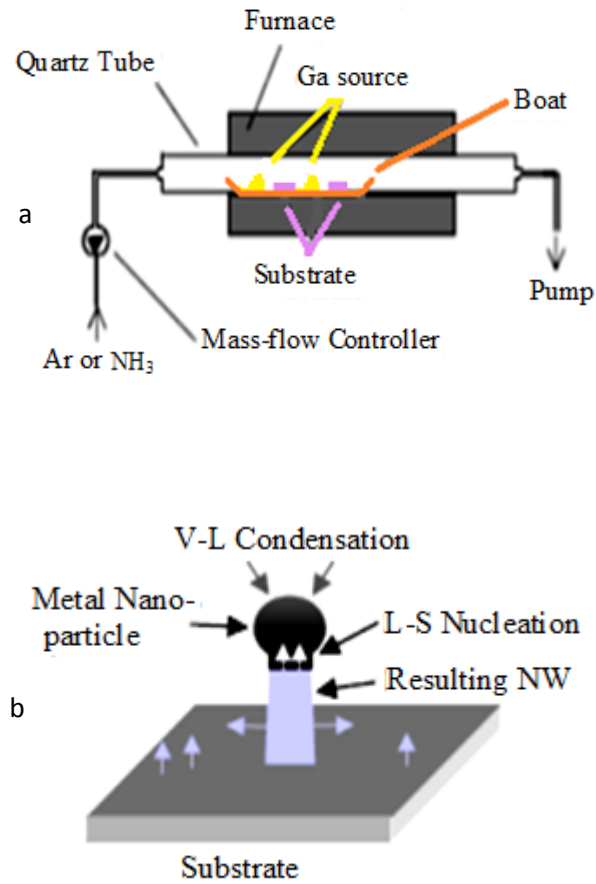


Figure 2.2: (a) Schematic of the CVD growth tube furnace with two substrates and a gallium source in a boat within the quartz tube. During growth, the tube is closed and linked to a pump, and NH₃ enters through a mass-flow controller. (b) Schematic diagram showing the suggested VLS growth mechanism. Ga and NH₃ vapor condense in the melted Ni or Fe nanoparticles (VL process) and then crystallize at the substrate (LS condensation) [39,40]

The nature of the growth procedure is based on the VLS mechanism as shown by Figure 2.2 (b). Although any growth system should avoid the use of toxic gases, such as ammonia, arsine, and phosphine, but CVD method usually involved the use of ammonia gas. However, this growth method is extraordinarily simple, compared with sophisticated methods such as MBE and MOCVD methods. This growth method has a potential to produce an extended variety of NWs, like group III–V binaries.

2.2.5 GaN NWs Grown by Laser-Assisted Catalytic Growth

Laser assisted growth is among the various methods developed to synthesize ultrathin NWs. The laser-assisted technique has unique advantages compared with other growth methods in synthesizing NWs containing compound chemical compositions since the number of elements involved is not important and the preparation of the target and the source materials in a crystalline form is also not essential. A usual mixture of the elements is suitable as the source material. These source materials are ablated to change to a vapor phase, which might have the same composition as the source materials. The vapor phase is then easily transferred to the substrate. A high-energy laser is capable to ablate solid materials in an extremely short time and vaporize the substances in a nonthermal equilibrium process. This technique is especially functional in the synthesis of NWs which have a high-melting temperature, such as of GaN and SiC. Furthermore, the laser-assisted technique is a very effective method in producing NWs with multiple components and in doping NWs during growth. The obtained vaporized molecules or clusters by the very high powered laser have very high kinetic energy, around 100 eV, which can enhance the chemical reaction, such as the reaction with oxygen, carbon or other gases. Therefore, the laser-assisted technique can largely improve the quality of the NWs at a low substrate temperature.

Figure 2.3 shows the experimental schematic setup of a laser-assisted technique. The laser used in this method can be an Nd:YAG laser, an excimer laser or any high-powered pulse laser. The overall evolution of NW growth using laser ablation is shown in Figure 2.4.

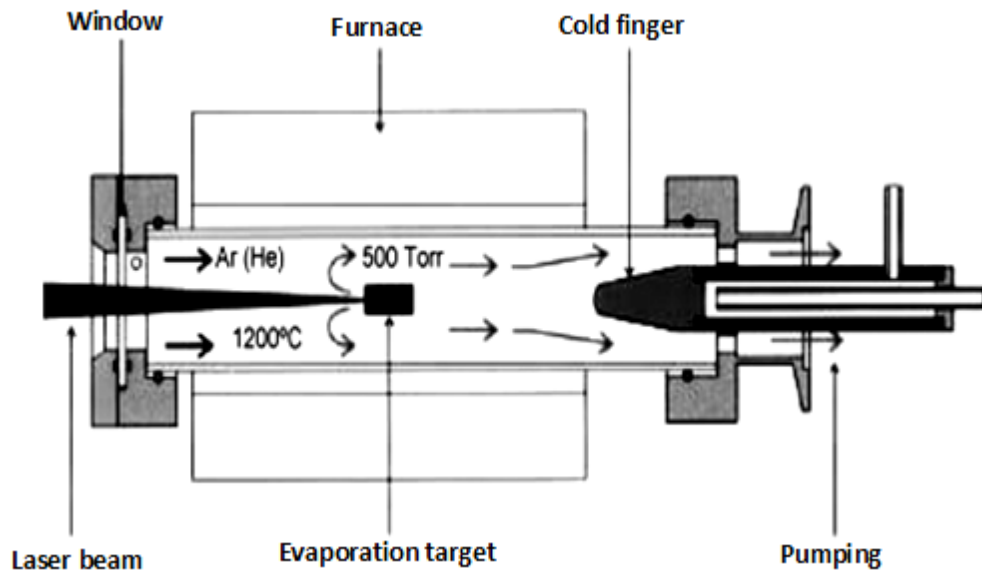


Figure 2.3: Experimental setup to synthesize GaN NWs by laser ablation (taken from Ref. [27])

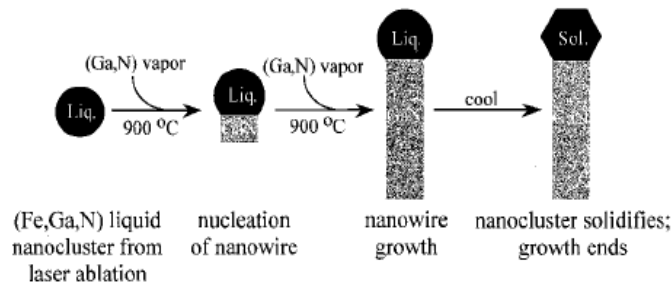


Figure 2.4. The overall evolution of NW growth following the production of the catalytic nanocluster using laser ablation (taken from Ref. [45])

2.2.6 GaN NWs Grown by Thermal Evaporation

To date, the growth of GaN NWs was mainly obtained by metal catalyst-assisted CVD process [42,43]. The usage of metal catalyst sometimes introduces impurities into GaN nanostructures and worsens the property of GaN-based nanodevices [48].

Therefore, the search to find some routines that avoid the employment of metal catalyst in growing GaN nanostructures is necessary. Although the MBE method has been proven successful in synthesizing high quality GaN NWs at low temperature, the low growth rate and yield is unsatisfactory. In addition, the MBE technique is also too

expensive for the production of GaN NWs for large scale commercial applications. In this study, the simple thermal evaporation technique that produces many different NWs with and without the use of a catalyst or template and even without lattice-matched substrates, has been used.

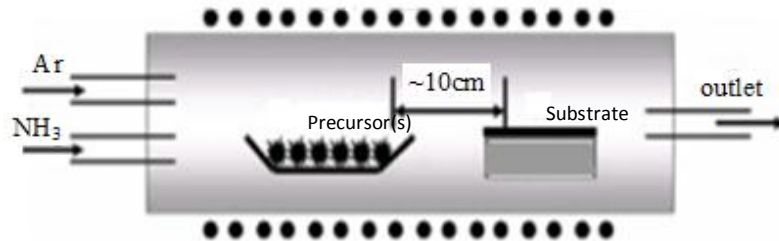


Figure 2.5: Scheme of the experimental-growth setup (taken from Ref. [49])

Nucleation at the initial stage may have the crucial role in both the in-plane and vertical alignments in the formation of GaN NWs. Without using metal catalyst, in this method, the nucleation can happen at any site of the substrate.

In contrast to the widely used VLS method, thermal evaporation is free from undesired contamination by strange metal atoms, which are usually used as VLS catalysts. Figure 2.5 shows the schematic diagram of the common thermal evaporation method.

In this method the composition could be grown without using catalyst, which is a remarkable advantage of this technique for NW growth. Furthermore, this technique can be used with many different kinds of substrates.

The typical materials suitable for thermal evaporation method are metal oxides, such as ZnO, SnO₂, and some semiconductors, such as GaN [12,66]. These NWs are fabricated through the evaporation of the materials' powders at high temperatures in an inert gas atmosphere or under a vacuum. NW products are formed in a low temperature

region ($<1150^{\circ}\text{C}$), where materials are laid down from the vapor phase. The NWs are assumed to be generated from the vapor phase through a process called VS growth.

The growth mechanisms of many NWs from thermal evaporation (without metal catalysts) are poorly understood [27]. Presently, thermal evaporation has produced a variety of long (up to 1 mm), uniform, single-crystal, and controlled NWs involving a growth mechanism very different from those of MOCVD and MBE.

2.2.6.1 Choice of Substrates

Addressing the lattice mismatch parameter problem is the main criterion in substrate selection. A number of materials, including Si (111), Si (100), Au-coated Si, GaN-Layer, and Al_2O_3 (sapphire), have been investigated as the substrates for GaN NWs growth. However, the lattice constants and the structure, composition, surface reactivity, surface treatment, as well as, electrical and chemical properties of the material, are also significant and have great influence in the selection of substrate materials, which can determine the crystal orientation, and surface morphology.

However, Si attracted attention as a substrate to grow GaN when the first MBE produced GaN LED in 1998 [50].

The lattice mismatch between GaN and Si is almost 16-17% (depends on the orientation of GaN structure and Si wafer) [51, 52], which makes a high dislocation density in grown GaN layers. Therefore, thick epilayers of GaN for device fabrication cannot be achieved without cracks, although it is achievable for thin GaN NWs. Si wafer is a potential substrate due to its wide availability, high quality, and low price. Both Si (100) and (111) have been employed for wurtzite GaN growth [53]. Si is also available with low resistivity (up to $10^4 \Omega\cdot\text{cm}$), which is less than GaN, SiC or sapphire, and may lead to the production of good quality electronic devices.

The gliding of the crystal over the porous layer can effectively lower the stress buildup during growth. This method has grown very high quality material. Stress was also reduced by some research groups through N implantation of Si (100) [50] as substrate and obtained good results. Therefore, the use of suitable substrates for growth of GaN NWs results in a good quality material.

Patterning substrates by etching or masking or the use of a buffer layer is another low cost and effective method to reduce the cracks or stress. Cracks or dislocations will be guided in the etched or masked layer and will result in low crack density or dislocations in the epitaxial layer [54].

However, sapphire has three reasons to refuse it as an “ideal material” when used in the construction of electronic devices based on GaN. These reasons are: 1) Its thermal expansion coefficient is higher than that of GaN, which leads to cracking of the films; 2) A rather big misfit of the substrate lattices (around 16%), which resulted in high number of defects; 3) It is an insulator, which is an additional exhausting engineering problem. As it cannot be a part of p-n junction.

Presently, remarkable intensive research for new substrate materials, which can be suitable for GaN relative to their lattices, electrical and thermal properties for GaN epitaxy growth, are carried out. Some physical properties of GaN nanostructure are promising as a semiconductor in many optoelectronic and electronic instruments [4,5]. The application of various porous layers, in particular, PSi, PGaN, and PZnO layers, are investigated in this research to solve the above problems.

2.2.6.2 Type of Gases as Carriers

The term “carrier gas” was first introduced by A. J. Martin, the inventor of chromatography of gases, who used it as a term for the mobile phase. This term is still

used as a synonym for a gaseous mobile phase. Any inert gas can be the carrier gas, such as helium (He), nitrogen (N₂), argon (Ar), and under certain situations hydrogen (H₂).

Helium gas is a minor component of natural gas. It must be purified from the natural gas, which causes less availability and high price of this carrier gas. Not only the price of He gas is high, but also it is a low density carrier gas [55].

The use of H₂ gas requires a vacuum chamber; otherwise, this gas will create hydrocarbons [56]. According to some researches on growing GaN NWs, N₂ is not as suitable carrier gas as Ar due to produce not uniform NWs [57]. Also N₂ gas is much more active compare to Ar and bonds with many metals (mercury, zinc, cadmium, magnesium) creating various nitrides as contamination during the growth in high temperature [58].

Ar is considered to be an inert or noble gas and does not affect the chemical composition of compounds. This gas is used for cutting, welding, and blanketing reactive components, and as a nonreactive atmosphere to grow semiconductor crystals [59]. Ar can replace air in most applications in a controlled atmosphere. Ultra-pure Ar is used to prevent the occurrence of impurities in the growth of semiconductors [60].

The creation of 1-D nanoscale building blocks with different shapes and sizes is critical for the nanotechnology procedure. Usually, NH₃ (or a mixture of NH₃ and Ar) is used to synthesize GaN NWs as carrier gas or precursors for nitrogen.

2.3 Solar Cell Based on Nitrides

The next sections discussed about solar cells based on Nitrides.

2.3.1 Thin Film Nitrides Solar Cell

Group III-nitride semiconductors have been greatly applied for fabrication of LEDs, laser diodes, heterojunction transistors, and photodetectors. With the combination of $\text{In}_x\text{Ga}_{1-x}\text{N}$, $\text{Al}_x\text{Ga}_{1-x}\text{N}$ and $\text{In}_x\text{Al}_y\text{Ga}_{1-(x+y)}\text{N}$ systems, the energy bands of the semiconductor's materials of the PV devices can be optimized, to absorb photon energy from 0.7 eV of the infrared to 6.2 eV of the ultraviolet regions. So a high-efficiency tandem solar cell in a single epitaxy system can be achieved.

$\text{In}_x\text{Ga}_{1-x}\text{N}$ alloys are both wide and direct-band-gap materials. Also the thicknesses of these epitaxial layers are not very important to yield enough IQE while generating photocurrents due to the high absorption coefficients ($\sim 10^5 \text{ cm}^{-1}$) near its energy band gap [61].

The thickness limit of high quality $\text{In}_x\text{Ga}_{1-x}\text{N}$, $\text{Al}_x\text{Ga}_{1-x}\text{N}$ and $\text{In}_x\text{Al}_y\text{Ga}_{1-(x+y)}\text{N}$ epitaxial layers grown on sapphire substrate is around hundreds of nanometers because of the large lattice mismatch between them, particularly for high-indium contained materials [62]. R. Islam et al. reported a conversion efficiency of 0.75% for $\text{In}_{0.25}\text{Ga}_{0.75}\text{N}$ n-p junction grown by MOVPE. They also said that these achievements indicate the potentiality of InGaN for future high performance solar cells [63].

Unfortunately, most of the reported InGaN thin films based solar cells have shown very low efficiency of less than 2% [58, 60]

J. Sheu et al. showed GaN/InGaN thin film solar cells with the device exhibiting an efficiency of 0.80% [64]. Recently research on quaternary $\text{Al}_{0.08}\text{In}_{0.08}\text{Ga}_{0.84}\text{N}$ solar cells indicates a high conversion efficiency of 9.74% [65].

The MQWs and superlattice schemes showed improved solar-cell performance, however, both schemes still have the disadvantage that the absorption layer is very thin to sufficiently absorb the sun rays. Some characterization results clearly indicate that usage of the mirror structure is beneficial for the absorption of a thin layer InGaN to enhance light absorption and, then, improves solar cell performance [64].

2.3.2 GaN NWs Solar Cell

Solar cells based on nanostructures can absorb more sunlight than solar cells based on conventional flat surfaces, which are commonly produced these days. In theory, scientists have calculated that the nanostructures have a higher absorbance in the high frequency region than their thin film counterparts, due to their less reflections of light. This kind of structure can absorb the photons incident directly on it and the photons scattered among its structure [62, 63]. Also the solar cell performance depends on the material used in the cell. Si and other conventional materials which have been widely used have smaller band gap compare to GaN.

In solar cells, the GaN NWs are grown on certain types of substrates, creating a surface that is able to absorb more sunlight than a flat surface, thus improving the efficiency of the cells [68]. These NWs also function as an antireflector to effectively reduce light loss for solar cell applications. Also there is the reduction in the amount of active materials consumed as compared to using thin films or bulk materials [69]. GaN NWs with bigger band gap than Si and other conventional solar cell materials, can absorb more high energy (blue and UV) sunlight and could have better conversion efficiencies as compared to thin films.

Vapor phase and chemical methods such as vapor phase epitaxy (VPE), chemical beam epitaxy (CBE), and molecular beam epitaxy (MBE), which are very expensive

and are not easy to do [23, 67]. As a result, the primary focus of current photovoltaic cell research is to find new methods and materials to improve device efficiency, cost, and safety.

2.3.3 Metal Contacts for Thin Film Nitrides Solar Cell

Metal contacts are applied, with their pattern on the surface of the cell defined by printing through a properly patterned emulsion screen or mask [71].

The external quantum efficiency will become much better by optimizing the top contact. Semitransparent ohmic contacts (Ni/Au) to GaN were coated by electron beam evaporation on the entire mesa and followed by rapid thermal annealing for 5 min. Some other contacts to GaN were formed by evaporating Al/Au and subsequent lift-off. No surface passivation or antireflection coating was used. The efficiency of these solar cells can be enhanced more by optimizing the GaN contact such as optimizing the Au and Ni thicknesses and exploring various contacts such as zinc oxide and indium tin oxide [65,66].

Other research groups have shown that metal contacts to GaN may cause huge band bending at the surface of the semiconductor. Also metal contacts have been used to increase the quality of the contact to GaN and AlGaN layers due to the increase in the depletion layer in the surface of the device, and some cells are covered with Ag nanoparticle arrays [60,67].

Figure 2.6 shows the schematic of the Ag/n-Al_xIn_yGa_{1-(x+y)}N/AlN(buffer)/p-Si/Au solar cell which indicates the thickness of each layer.

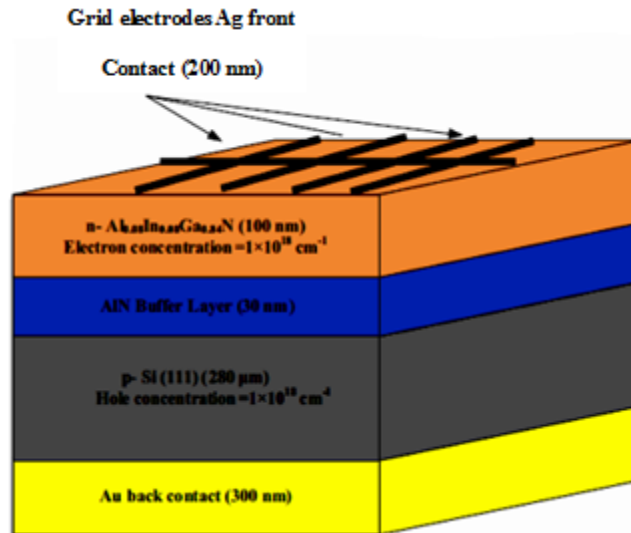


Figure 2.6: Schematic of the Ag/n- $\text{Al}_x\text{In}_y\text{Ga}_{1-(x+y)}\text{N}$ /AlN(buffer)/p-Si/Au solar cell. (taken from Ref.[74])

The reaction at the Si/AlN or Si/GaN interface will form a thin layer of SiN. This process can lead to form nitrogen vacancies, which yield highly doped interface, resulting in the ohmic contact formation [74].

2.4 Summary

This chapter has reviewed about different growth techniques of GaN NW, such as MBE, HVPE, MOCVD, CVD, Laser-Assisted Catalytic Growth and Thermal Evaporation. It also described the choice of substrates and gases which were used in this work. Finally it explained about the Solar cells based on Nitrides.